Detection of small fires from NOAA/AVHRR data

Yu.V. Gridnev

Institute of Atmospheric Optics,
Siberian Branch of the Russian Academy of Sciences, Tomsk

Received January 24, 2002

A new algorithm for detection of small-sized fires from five-channel NOAA/AVHRR data is developed, implemented, and tested. A peculiarity of the algorithm is the use of a phenomenological model for description of small-sized fires at a subpixel level and interfering factors like cloud patches. Some examples of algorithm operation for detection of fires at the territory of the Tomsk Region are presented.

Detection of small-sized fires from AVHRR data is a complicated problem because of the low resolution of space images that is, at best, 1.1 × 1.1 km, nonstationary optical and geometrical conditions of observation of the Earth's surface, and stochastic cloud fields giving rise to artifacts.[1,2] In fact, we deal with development of an algorithm for detection of "heated" pixels in chaos of various data on radiative temperature and various conditions of vision through the atmosphere. A large number of papers are devoted to detection of fires, but ideologically they are represented by two classes of algorithms. In the first class, the decision rules of detection algorithms form thresholds based on some physical reasons in the form of inequalities.[1] In the second one, the optimal decision rules are constructed based on the knowledge of the probability distributions of observations in different situations. In this paper, the emphasis is on the construction of indicator spaces through nonlinear transformation of the initial description, in which the decision rule for detection has the simplest form.

Consider first the problem of detection of thermal anomalies in the case that a scanner aperture records a 1.1 × 1.1 km surface element only partly occupied by a fire. In this case, the radiative temperature of the corresponding pixel consists of the background temperature and the temperature of a hot part taken in proportion to the occupied areas.

1. Detector of temperature anomalies

To detect hot surface areas within the scanner aperture, we will use the ratio of intensities in the AVHRR channels 3, 4, and 5 based on the following obvious reasons. Assume that some surface region with the area S corresponding to the radiometer field of view and the background temperature T_0 includes a hot part with the area S_1 and the temperature T_1. We believe that both the cold and the hot parts of the region correspond to the black body model. In this case, the radiation intensity is the weighted sum of intensities of the cold and hot parts determined by Planck's formula:

$$I(\nu) = \alpha \frac{C_1 \nu^3}{\exp(C_2 \nu/T_0) - 1} + \beta \frac{C_1 \nu^3}{\exp(C_2 \nu/T_1) - 1}, \quad (1)$$

where $\alpha = (S - S_1)/S$ and $\beta = S_1/S$ are weighting factors; $C_1 = 1.1910659 \cdot 10^{-5}$ mW $(\text{m}^2 \cdot \text{sr} \cdot \text{cm}^{-4})^{-1}$, $C_2 = 1.438833$ cm · K.

The frequency dependence of the radiation for the temperatures $T_0 = 273$ K, $T_1 = 1273$ K and $S_1/S = 0.006$ is plotted in Fig. 1.

Let I_3, I_4, and I_5 be the intensities in the AVHRR channels 3, 4, and 5, respectively.

To reduce the intensities in different channels to the same scale, we introduce the normalization coefficients C_3 and C_5 as

$$C_3 = I_4(323)/I_3(323),$$

$$C_5 = 0.845\, I_4\,(323)/I_5(323),$$

where $I_3(323)$, $I_4(323)$, and $I_5(323)$ are the intensities in the channels 3, 4, 5 at the temperature of 323 K as calculated from radiometer spectral characteristics.

Then we construct the following parameters:

$$R = 50\left(1 - \frac{C_5 I_5}{I_4}\right); \; G = 5\frac{C_5 I_5}{I_4};$$

$$B = \frac{C_3 I_3}{I_4},$$

which form some manifold of the three-dimensional space. In the *RGB* space, we turn into the plane (x, y) passing through unit points of the coordinate system introduced, that is, find the point of intersection of the vector (R, G, B) and the plane passing through the points (1, 0, 0), (0, 1, 0), and (0, 0, 1).

Let

$$r = \frac{R}{R+G+B}, \quad g = \frac{G}{R+G+B}, \quad b = \frac{B}{R+G+B},$$

$$x = \frac{b-g}{\sqrt{2}}, \quad y = \frac{3r-1}{\sqrt{6}}. \quad (2)$$

0235-6880/02/08 659-04 $02.00

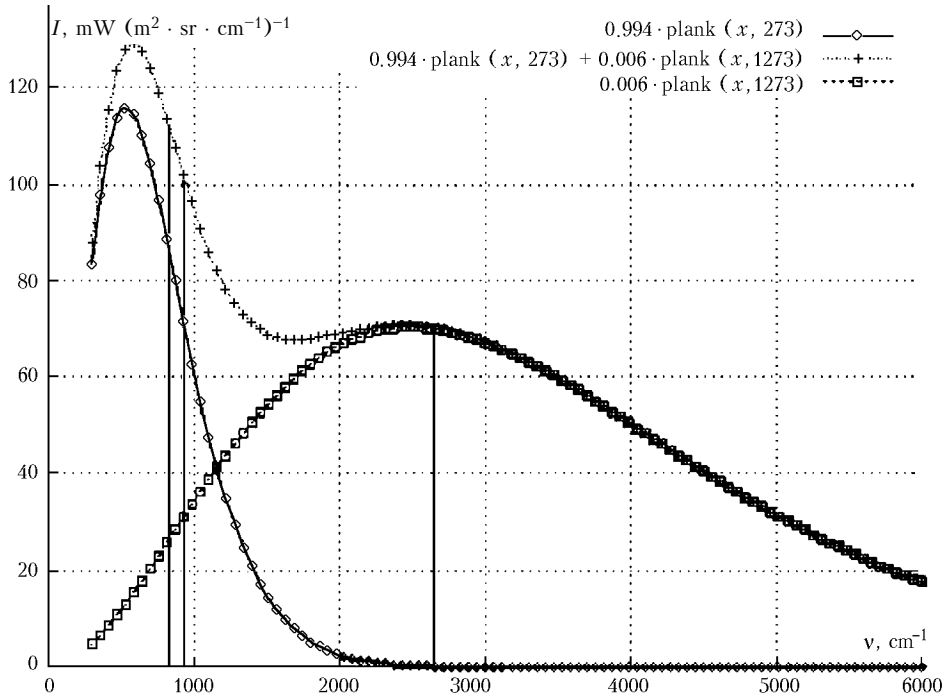

Fig. 1. Frequency dependence of radiation for the temperatures T_0 and T_1.

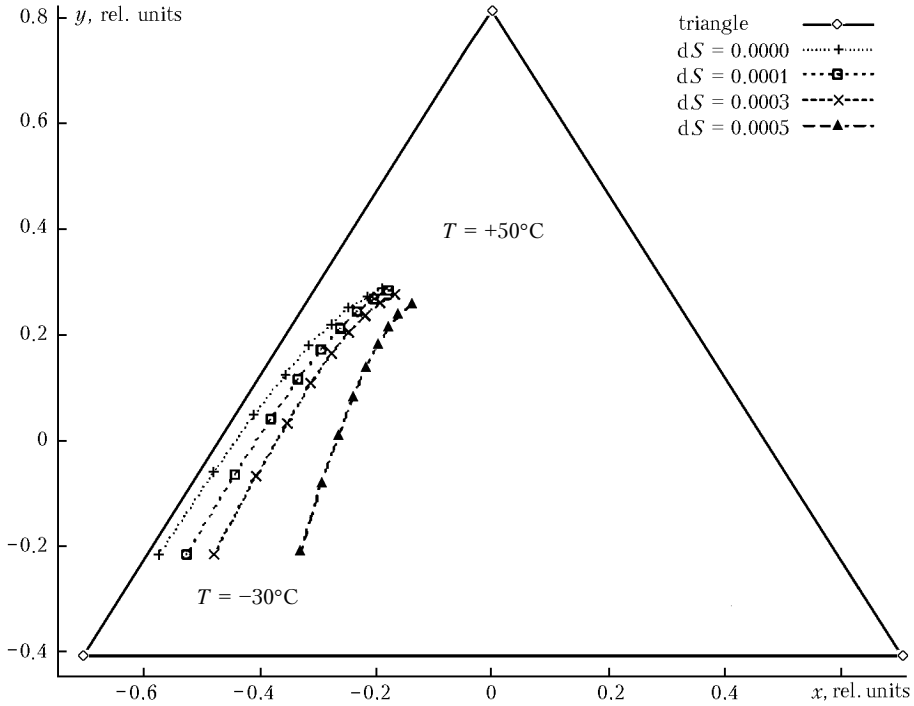

Fig. 2. *RGB* plane of the indicator space for detection of thermal anomalies.

The decision rule in the plane (x, y) is formed based on the following grounds:

– in the absence of hot parts, the points (x, y), generated by the transformed values of the radiative temperatures in the channels 3–5 fall on some curve that will be called the basic one;

– when a hot part appears, the corresponding point shifts down to the right depending on its size.

The corresponding curves for the background temperature T varying from −30 to +50°C are exemplified in Fig. 2.

The curves were calculated for NOAA-14 at the hot part temperature of 773 K (500°C) and hot part contributions (in relative areas) of 0.0001, 0.0003, and 0.0005. For NOAA/AVHRR, this corresponds to the linear dimensions of the hot part of roughly 10, 17, and

22 m^2, respectively, at nadir point. Unfortunately, the efficiency of this decision rule is insufficiently high because of frequently occurring flares that are easily recognized as fires.

2. Allowance for interfering factors

The main factor leading to false detection of hot parts in daytime is the solar radiation scattering by clouds. Let estimate the scattered solar radiation as some additive:

$$I_3 = I_{3c}(T_4) + \Delta I,$$

where I_3 is the intensity in the channel 3; $I_{3c}(T_4)$ is the intensity calculated from the temperature of the channel 4; ΔI is an additive due to the scattered solar radiation.

Let us connect the estimated solar additive with the albedo in the channel 1 and the temperature difference between the channels 4 and 5 through:

$$\Delta I = f(A_1)\ [1 + k_{45}\ (T_4 - T_5)]. \qquad (3)$$

Here $f(A_1)$ is the additive dependence on the albedo in the channel 1; k_{45} is the coefficient of additive relation with the temperature difference between the channels 4 and 5.

Since we failed to reveal a unique dependence between the solar additive and the albedo in the channel 1 and the temperature difference between the channels 4 and 5, we estimate the unknowns entering into Eq. (3) in some vicinity of the analyzed point. First, we estimate the coefficient k_{45}. For this purpose, using the data of the channels 1, 4, and 5, compile the table of additive dependence on the temperature difference and the albedo in the channel 1 with the step of 1% in albedo and 0.5 degrees in temperature. We assume that this table has n values of the albedo and m values of the temperature difference. Using this table, we estimate the coefficient k_{45} by the least-square method for those albedo values, for which values exist in a rather large temperature range:

$$\Delta I = I_3 - I_{3c}(T_4),\ \ \Delta I = K_{45j}\ (T_4 - T_5) + \Delta I_0,$$

$$\frac{\Delta I}{\Delta I_0} = \frac{K_{45j}}{\Delta I_0}\,\Delta T + 1,\ \ \frac{\Delta I}{\Delta I_0} = k_{45j}\,\Delta T + 1.$$

For each column of the table, calculate

$$k_{45j} = \frac{n\sum_{i=1}^{n}\Delta T_i \Delta I_i - \sum_{i=1}^{n}\Delta T_i \sum_{i=1}^{n}\Delta I_i}{\sum_{i=1}^{n}\Delta I_i \sum_{i=1}^{n}\Delta T_i^2 - \left(\sum_{i=1}^{n}\Delta T_i\right)^2},\ j = 1, \ldots, m. \qquad (4)$$

Finally, after averaging of the obtained values, we have

$$k_{45} = \frac{1}{m}\sum_{j=1}^{m} k_{45j}\ . \qquad (5)$$

The function $f(A_1)$ is estimated based on the two-dimensional histogram of the normalized solar additive $h(A_1, \Delta I_r)$ with the ranges of albedo and additive values divided into 100. First, we determine the minimal $\Delta I_{\min j}$ and maximal $\Delta I_{\max j}$ values of the additive for each albedo interval $j = 1, \ldots, m$, from which we can calculate the normalization coefficients:

$$k_{rj} = \frac{100}{\Delta I_{\max j} - \Delta I_{\min j}}\ .$$

Then, for each albedo interval, we can find the normalizing additive with allowance for the predetermined dependence on the temperature difference between the channels 4 and 5:

$$\Delta I_j = I_3 - I_{3c}(T_4),$$

$$\Delta I_{rj} = k_{rj}\left(\frac{\Delta I_j}{1 + k_{45}(T_4 - T_5)} - \Delta I_{\min j}\right),\ j = 1, \ldots, m. \qquad (6)$$

Using the obtained values of ΔI_{rj} and albedo A_1 in the channel 1, we can draw the two-dimensional histogram $h(A_1, \Delta I_{rj})$, from which we can determine the values of $\Delta I_{rj0.85}$ at the level of 0.85 and the rms deviation σ_j of the additive ΔI_{rj} for each albedo interval. From the obtained values, we construct the function of additive dependence on the albedo in the channel 1, assuming $A_1 = j$:

$$f(A_1) = \Delta I_{\min j} + \frac{\Delta I_{rj0.85} + \sigma_j}{k_{rj}}\ .$$

Intermediate values can be obtained by means of linear interpolation. Then the intensity in the channel 3 is corrected with the use of the obtained estimate:

$$I_{3k} = I_3 - f(A_1)\ [1 + k_{45}\ (T_4 - T_5)], \qquad (7)$$

and analysis for the presence of a hot point is carried out with the use of the detector described above.

3. Experiments on detection of thermal anomalies

The program for fire detection was implemented in the form of a Windows 95 console application. Its input data are the HRPT file generated by the SX Recevier application of the SCANEX station and the NORAD-TLE file of orbiting elements. Thus, the initial data were five-channel NOAA/AVHRR data in the form of images received four to five times a day for the territory of the Tomsk Region.

The detection algorithm operated in the automatic mode, and the results of the analysis in the form of BMP images of the region under study with the separated thermal anomalies and color indication of the temperature scale of fires was saved on the hard disk.

The accompanying text file contains the information about the latitude and longitude of each detected anomaly, the number of pixels occupied by a fire, and the value of its temperature power.

The information on the fires detected in the monitoring mode was sent to fire protection services of the Tomsk Region.[3,4] The efficiency of fire detection in this case was somewhat higher than the efficiency of an operator experienced in detection of fires.

References

1. G.A. Zherebtsov, V.D. Kokurov, V.V. Koshelev, and N.P. Min'ko, Issled. Zemli iz Kosmosa, No. 5, 74–77 (1995).
2. V.V. Belov, S.V. Afonin, Yu.V. Gridnev, and K.T. Protasov, Atmos. Oceanic Opt. **12**, No. 10, 951–956 (1999).
3. S.V. Afonin, V.V. Belov, and Yu.V. Gridnev, Atmos. Oceanic Opt. **13**, No. 11, 921–929 (2000).
4. S.V. Afonin and V.V. Belov, Atmos. Oceanic Opt. **14**, No. 8, 634–638 (2001).